

Analyses of features of magnetic cycles at different amounts of dynamo supercriticality: Solar dynamo is about two times critical

Sanket Wavhal¹ · Pawan Kumar^{1,2} · Bidya Binay Karak¹

© The author(s)

Abstract The growth of a large-scale magnetic field in the Sun and stars is usually possible when the dynamo number (D) is above a critical value D_c . As the star ages, its rotation rate and thus D decrease. Hence, the question is how far the solar dynamo is from the critical dynamo transition. To answer this question, we have performed a set of simulations using Babcock–Leighton type dynamo models at different values of dynamo supercriticality and analyzed various features of magnetic cycle. By comparing the recovery rates of the dynamo from the Maunder minimum and statistics (numbers and durations) of the grand minima and maxima with that of observations and we show that the solar dynamo is only about two times critical and thus not highly supercritical. The observed correlation between the polar field proxy and the following cycle amplitudes and Gnevyshev-Ohl rule are also compatible with this conclusion.

Keywords: Solar dynamo; convection zone; magnetic field; solar cycle; sunspot

1. Introduction

Observations show that the Sun and Sun-like stars exhibit variable large-scale magnetic fields. This variation in the magnetic fields can be best seen in the form of irregular amplitude, grand minima and maxima, Gnevyshev-Ohl rule, Gnevyshev peaks (Wright, 2016; Shah et al., 2018; Karak, Mandal, and Banerjee, 2018;

✉ S. Wavhal
wavhal.sankets.phy20@itbhu.ac.in

✉ P. Kumar
pawan.kumar.rs.phy18@itbhu.ac.in, pawankumar@iiap.res.in

✉ B.B. Karak
karak.phy@itbhu.ac.in

¹ Department of Physics, Indian Institute of Technology (BHU) Varanasi 221005, India

² Indian Institute of Astrophysics, Koramangala, Bengaluru, 560034, India

Garg et al., 2019; Usoskin, 2023; Karak, 2023). For the Sun, these characteristics can be observed in the last 400 years sunspot data and its proxy, such as ^{10}Be and ^{14}C data of 11,000 years (Usoskin, 2023; Biswas et al., 2023). Observational studies suggest a variation in the large-scale surface magnetic field of stars with its age which is known as ‘magnetochronology’ (Vidotto et al., 2014). Moreover, studies (Skumanich, 1972; Rengarajan, 1984; Noyes et al., 1984) show that the younger stars rotate faster and show much more magnetic activity than older stars. Thus, the rotation rate (or period) largely controls the magnetic activity of Sun and Sun-like stars which is connected with their ages.

Therefore, there must be a critical age or rotation period for stars beyond which the generation of large-scale magnetic fields ceases. We note that the large-scale magnetic field is produced above the critical dynamo transition and, in some cases, in subcritical regimes (Kitchatinov and Olemskoy, 2010; Karak, Kitchatinov, and Brandenburg, 2015; Vashishth, Karak, and Kitchatinov, 2021). However, the appealing question is, ‘at what regime is our solar dynamo operating, or in other words, how far is our Sun from the critical dynamo transition? Observational study of Metcalfe, Egeland, and van Saders (2016) reveals that the solar dynamo may be in the transition region of magnetically active and inactive branches of stars. Theoretical modelings (Cameron and Schüssler, 2017, 2019; Tripathi, Nandy, and Banerjee, 2021) indicate that the solar dynamo is possibly near the transition to a magnetically inactive state. Furthermore, Kitchatinov and Nepomnyashchikh (2017) showed that the solar dynamo is only about 10% supercritical. Thus, this indicates that the solar dynamo is operating near the critical dynamo transition. Recently, Ghosh et al. (2024) showed that the solar dynamo is not highly supercritical and operating near the dynamo’s critical regime based on the nonlinear characterization of solar magnetic cycles. In the present manuscript, by conducting independent studies, we provide additional support that the solar dynamo operates only in the weakly supercritical regime.

The large-scale magnetic fields of the Sun and Sun-like stars are believed to be the manifestation of the dynamo process operating in their convection zones (CZs) (Moffatt, 1978; Parker, 1955). In the $\alpha\Omega$ -type dynamo, which applies for the Sun, the important controlling parameter is the dynamo number D . The magnetic field grows when D exceeds a critical value. Here, D can be defined as

$$D = \frac{\alpha_0 \Delta\Omega L^3}{\eta_0^2}, \quad (1)$$

where $\Delta\Omega$ is angular velocity variation within CZ, α_0 is the measure of the α effect, L is the depth of CZ, and η_0 is the turbulent magnetic diffusivity. In the classical $\alpha\Omega$ type dynamo, helical convective α generates the poloidal field from the toroidal field (e.g, Krause and Rädler, 1980). However, in recent years, it has been realized that the generation of the poloidal field takes place due to the decay and dispersal of the tilted bipolar magnetic regions known as Babcock–Leighton mechanism (Babcock, 1961; Leighton, 1969), which is strongly supported by observations (Dasi-Espuig et al., 2010; Kitchatinov and Olemskoy, 2011; Mordvinov et al., 2022; Cameron and Schüssler, 2015, 2023). Babcock–Leighton type models have emerged as a popular paradigm for explaining various features of

regular solar magnetic cycle including the polarity reversals, poleward migration of surface magnetic field, and the equatorward migration of toroidal field (Karak et al., 2014; Charbonneau, 2020; Cameron and Schüssler, 2023). As in this model, the decay of tilted bipolar magnetic regions (BMR) generates the poloidal field on the solar surface, we have a good observational back up of this part of the model. By monitoring the build-up rate of the polar field after its reversal (Kumar, Biswas, and Karak, 2022; Biswas, Karak, and Kumar, 2023) or by feeding the peak polar field information into a dynamo model (e.g., Schatten et al., 1978; Choudhuri, Chatterjee, and Jiang, 2007; Bhowmik and Nandy, 2018; Hazra and Choudhuri, 2019; Kumar et al., 2021), one can predict the amplitude of the next solar cycle. One good thing about these models is that the fluctuations in the BMR properties are observed and thus quantified (Jiang, Cameron, and Schüssler, 2014; Olemskoy, Choudhuri, and Kitchatinov, 2013; Kumar, Karak, and Sreedevi, 2024; Sreedevi et al., 2024). These fluctuations in the Babcock–Leighton dynamo models explain majority of the irregular features of solar cycle, including long-term modulation and grand minima (Charbonneau and Dikpati, 2000; Charbonneau, Blais-Laurier, and St-Jean, 2004; Choudhuri and Karak, 2009, 2012; Karak, 2010; Olemskoy and Kitchatinov, 2013; Passos et al., 2014; Karak and Miesch, 2017, 2018). Recently, Babcock–Leighton dynamo model has also been used to explore the features of stellar magnetic variability (Vashishth, Karak, and Kitchatinov, 2023).

In recent years, global MHD simulations are producing encouraging results of the solar magnetic field and some large-scale flows such as solar-like differential rotation and meridional flow in some parameter regimes (e.g., Brun, Miesch, and Toomre, 2004; Racine et al., 2011; Fan and Fang, 2014; Karak et al., 2015; Augustson et al., 2015; Käpylä et al., 2016; Brun et al., 2017; Karak, Miesch, and Bekki, 2018; Strugarek et al., 2018; Brun et al., 2022; Hotta, Kusano, and Shimada, 2022). However, these simulations are still far from producing many features of surface magnetic field and deep convection (Brun and Browning, 2017; Käpylä et al., 2023). Despite these, one still could employ global MHD simulation to identify the supercriticality of the Sun as the flows are self-consistently generated in the model and all nonlinearities are by default captured. However, we are not doing this because of two reasons. The first is because we need to run these simulations for several thousands of years to analyse the long-term modulation and grand minima, which is notoriously expensive numerically, and the second is due to difficulties in changing the dynamo number by keeping the critical dynamo transition point unaltered in global simulations.

Previous studies demonstrate that the variability of the magnetic cycle depends on the supercriticality of the dynamo (Charbonneau, St-Jean, and Zacharias, 2005; Karak, Kitchatinov, and Brandenburg, 2015; Charbonneau, 2020; Karak, 2023). Thus, changes in the supercriticality of the dynamo, will cause change in the features of the solar cycle, including the properties of grand minima and maxima and the memory of the polar field (Kumar, Karak, and Vashishth, 2021). Therefore, in this manuscript, we have estimated the solar dynamo supercriticality by analysing various features of magnetic cycle and comparing them with observations. To do so, we have used several dynamo models, namely the Babcock–Leighton dynamo models used in Kumar, Karak, and Vashishth

(2021) and Passos et al. (2014) and the time delay models of Hazra, Passos, and Nandy (2014) and Albert et al. (2021). We identify the regime of solar dynamo operation by estimating the recovery rate of Maunder Minimum (Section 3.1) and statistics of grand minima and maxima (Section 3.2). We conclude that the features of solar cycle favour weakly supercritical solar dynamo. We also make comments on whether the linear correlation between the available proxy of the polar field and next cycle amplitudes (Section 3.3.1) and the Gnevyshev-Ohl rule (Section 3.3.2) can be used to offer further support for our conclusion.

2. Models

We use various Babcock–Leighton type flux transport and time delay dynamo models to conduct this study. Below we briefly discussed these models.

2.1. Flux transport dynamos

For the flux transport dynamo model (Choudhuri, Schüssler, and Dikpati, 1995; Karak et al., 2014; Hazra et al., 2023), we solve the following equations for axisymmetric magnetic field:

$$\frac{\partial A}{\partial t} + \frac{1}{s}(\mathbf{v} \cdot \nabla)(sA) = \eta_p \left(\nabla^2 - \frac{1}{s^2} \right) A + S_\alpha, \quad (2)$$

$$\frac{\partial B}{\partial t} + \frac{1}{r} \left[\frac{\partial (rv_r B)}{\partial r} + \frac{\partial (v_\theta B)}{\partial \theta} \right] = \eta_t \left(\nabla^2 - \frac{1}{s^2} \right) B + s(\mathbf{B}_p \cdot \nabla)\Omega + \frac{1}{r} \frac{d\eta_t}{dr} \frac{\partial}{\partial r} (rB), \quad (3)$$

where A is the potential of poloidal magnetic field and B is the toroidal magnetic field, $s = r \sin \theta$ with θ being colatitude, $\mathbf{v} = v_r \hat{\mathbf{e}}_r + v_\theta \hat{\mathbf{e}}_\theta$ is the meridional circulation, Ω is the angular velocity, η_p and η_t are the turbulent diffusivities of the poloidal and toroidal fields, respectively, α is the parameter that captures the Babcock–Leighton process for the generation of the poloidal field from the toroidal one. In this study, we use three Babcock–Leighton models, namely Models I, II, and III.

For Models I and II we use a nonlocal α , which was used in earlier studies (Dikpati and Charbonneau, 1999; Choudhuri, Nandy, and Chatterjee, 2005; Choudhuri and Hazra, 2016). Thus, in these models,

$$S_\alpha = \frac{\alpha}{1 + \left(\frac{B(0.7R_\odot, \theta)}{B_0} \right)^2} B(0.7R_\odot, \theta), \quad (4)$$

where α is given by

$$\alpha = \frac{\alpha_0}{4} \sin \theta \cos \theta \left[\frac{1}{1 + e^{-\gamma(\theta - \frac{\pi}{4})}} \right] \left[1 + \operatorname{erf} \left(\frac{r - 0.95R_\odot}{0.05R_\odot} \right) \right] \left[1 - \operatorname{erf} \left(\frac{r - R_\odot}{0.01R_\odot} \right) \right] \quad (5)$$

where $\gamma = 30$ and α_0 is the amplitude of α effect. When we introduce fluctuations in these models, we multiply α_0 by a Gaussian of unity mean and 2.67 standard deviation as inspired by the study of Olemskoy, Choudhuri, and Kitchatinov (2013) using sunspot Catalog of Solar Activity of the Pulkovo Observatory. Also, for diffusivity, in these models, we consider $\eta_t = \eta_p = \eta$, where

$$\eta(r) = \eta_{RZ} + \frac{\eta_0}{2} \left[1 + \operatorname{erf} \left(\frac{r - 0.7R_\odot}{0.02R_\odot} \right) \right] + \frac{\eta_{\text{surf}}}{2} \left[1 + \operatorname{erf} \left(\frac{r - 0.9R_\odot}{0.02R_\odot} \right) \right], \quad (6)$$

where $\eta_{RZ} = 5 \times 10^8 \text{ cm}^2 \text{ s}^{-1}$ and $\eta_{\text{surf}} = 2 \times 10^{12} \text{ cm}^2 \text{ s}^{-1}$. For Model I, we have considered $\eta_0 = 5 \times 10^{10} \text{ cm}^2 \text{ s}^{-1}$, and for Model II, we have used five times less diffusivity than in Model I.

Besides these models, we have also used the model of Passos et al. (2014) in which a weak mean-field α effect (Parker, 1955) is included in addition to the usual Babcock–Leighton source for the poloidal field (local prescription for α) and total poloidal field source considered as $S_\alpha = \alpha B$. Hence the total α effect in this model is defined as $\alpha = \alpha_{BL} + \alpha_{MF}$. Here,

$$\begin{aligned} \alpha_{BL} = \alpha_{0BL} \frac{\cos \theta}{4} \left[1 + \operatorname{erf} \left(\frac{r - 0.95R_\odot}{0.025R_\odot} \right) \right] \left[1 - \operatorname{erf} \left(\frac{r - R_\odot}{0.025R_\odot} \right) \right] \\ \times a_1 \left[1 + \operatorname{erf} \left(\frac{B_\phi^2 - B_{1lo}^2}{d_3^2} \right) \right] \left[1 - \operatorname{erf} \left(\frac{B_\phi^2 - B_{1up}^2}{d_4^2} \right) \right], \end{aligned} \quad (7)$$

with $B_{1lo} = 10^3 \text{ G}$, $B_{1up} = 10^5 \text{ G}$, $d_3 = 10^2 \text{ G}$, and $d_4 = 10^6 \text{ G}$ and $a_1 = 0.393$ is the normalization constant. α_{0BL} determines the amplitude of the Babcock–Leighton α coefficient, whose value is varied to change the supercriticality of the dynamo. Note that in addition to the upper quenching, there is a lower quenching of Babcock–Leighton effect, which becomes important when the toroidal field falls below 10^3 G in this model. This lower cut-off may not be well justified because BMRs do not show any cut-off in the field strength, and even the small BMRs show some systematic tilt, although the scatter around Joy’s law increases with the decrease of flux in the BMR (Jha et al., 2020; Sreedevi et al., 2024). However, as we are using the model of Passos et al. (2014) as it is, we are following the same procedure of lower quenching. Then, this model also includes a mean-field α , which operates at the weak field regime. As argued by Passos et al. (2014), when the magnetic field becomes weak during grand minima and Babcock–Leighton α is inefficient, this additional α helps recover the model from grand minima. The mean-field α is given by,

$$\alpha_{MF} = \alpha_{0MF} \frac{\cos \theta}{4} \left[1 + \operatorname{erf} \left(\frac{r - r_1}{r_2} \right) \right] \left[1 - \operatorname{erf} \left(\frac{r - R_\odot}{r_2} \right) \right] \frac{1}{\left[1 + \left(\frac{B_\phi}{B_0} \right)^2 \right]}, \quad (8)$$

with $\alpha_{0MF} = 0.4$, which determines the amplitude of the mean-field α , $r_1 = 0.713R_\odot$, $r_2 = 0.025R_\odot$, and $B_0 = 10^4 \text{ G}$. We introduce stochastic fluctuations in this model by replacing α with $\alpha(1 + f\sigma(t, \tau_{\text{cor}}))$, where σ is a uniform random

deviation within $[-1, 1]$ interval, τ_{cor} is the time interval after which α_0 is updated, and f is the percentage level of fluctuations.

We note that in this model, different values of diffusivity for the poloidal (η_p) and the toroidal field (η_t) are used; see Figure 7, right panel. The toroidal field diffusivity in the bulk of the CZ is about 50 times smaller than that of poloidal field. The justification for this is that the strong toroidal field remains confined in localized regions and experiences more quenching compared to the poloidal one, which remains spread (see Chatterjee, Nandy, and Choudhuri, 2004, where this idea was introduced).

The meridional circulation profile of this model is the same as used in the previous models, except the parameter v_0 whose value is taken to be -29 m s^{-1} in this model. For the other details of this model, we refer readers to Passos et al. (2014). We call this model as Model III. We note that for all the models, the angular frequency Ω is taken from an analytic approximation of the helioseismic data used in most kinematic dynamo models, precisely Equation 4 of Dikpati and Charbonneau (1999). Finally, we have used two other models, namely Models IV and V, which are time delay dynamo models as described below.

2.2. Time delay dynamo

In time delay dynamo model (Wilmot-Smith et al., 2006), we solve the following two truncated (removing all spatial dependence and taking into account the spatial segregation in the source regions) equations,

$$\frac{dB(t)}{dt} = \frac{\omega}{L}A(t - T_0) - \frac{B(t)}{\tau_d}, \quad (9)$$

$$\frac{dA(t)}{dt} = \alpha_0 f_0(B(t - T_1))B(t - T_1) - \frac{A(t)}{\tau_d}, \quad (10)$$

where ω and L represent the differential rotation and length scale in the tachocline, respectively, τ_d denotes the diffusion timescale of the turbulent diffusion in the CZ, while α_0 is the amplitude of the α -effect, similar to those used in flux-transport dynamo models. The parameters T_0 and T_1 account for the time delay in the conversion of the poloidal field into the toroidal field and vice versa. The factor f_0 is a quenching factor, which is approximated here by a nonlinear function:

$$f_0 = \frac{1}{4} [1 + \text{erf}(B^2(t) - B_{\text{min}}^2)] [1 - \text{erf}(B^2(t) - B_{\text{max}}^2)], \quad (11)$$

where B_{max} and B_{min} are the upper and lower limit to the toroidal field strength between which the α -effect can act (same as the previous model).

For Model IV, we follow Hazra, Passos, and Nandy (2014) with additional weak mean field poloidal source in the equation (10) similar to Model III. Thus equation (10) modified as,

$$\frac{dA(t)}{dt} = \alpha_0 f_0(B(t - T_1))B(t - T_1) + \alpha_{mf} f_1(B(t - T_2))B(t - T_2) - \frac{A(t)}{\tau_d}, \quad (12)$$

where $\alpha_{mf} = 0.2$, is the mean-field poloidal source and f_1 is the corresponding quenching which is given by,

$$f_1 = \frac{1 - \operatorname{erf}(B^2(t - T_2) - B_{eq}^2)}{2} \quad (13)$$

with $B_{eq}^2 = 1$ and $T_2 = 0.25$, is the time delay that is necessary for the toroidal field to enter the source region where the additional weak-field α effect is located. The variation of the quenching profile f_0 and f_1 is shown in Figure 8. We take $\tau_d = 15$, $B_{min} = 1$, $B_{max} = 7$, $T_1 = 0.5$, $T_0 = 2$, and $\omega/L = -0.34$ for this model.

Finally for Model V, we follow Albert et al. (2021), and take following values of the parameters: $\alpha_{mf} = 0$ (no mean-field α), $B_{min} = 1$, $B_{max} = 10$, $\tau_d = 1$, and $(T_0 + T_1)/\tau_d = 0.82$. In this model, the quenching profile is similar to f_0 except for the upper and lower cut-off values of the magnetic field and is presented as f' in Figure 8 in the Appendix. For these two models (IV and V), we incorporate stochastic fluctuations in α_0 and α_{mf} in the same way as in Model III.

3. Results and Discussion

In all the dynamo models used in our studies, the amplitude of the α coefficient, α_0 , determines the dynamo efficiency. Growing magnetic field, i.e., dynamo action, is possible only when the value of α_0 exceeds a certain value, which is defined as α_0^{crit} . Its value is obviously different for different models, which is given in the first column of Table 1. Thus, we define a quantity, $\hat{\alpha}_0 = \alpha_0/\alpha_0^{crit}$, which can be a measure of the amount of dynamo supercriticality. As we increase the value of $\hat{\alpha}_0$ beyond unity, the model becomes more and more supercritical. We note that this $\hat{\alpha}_0$ is not exactly the dynamo number, which can have complicated dependence on parameters in the present flux transport dynamo models (unlike Eq. 1 for simple $\alpha \Omega$ dynamo model) but it is related to it. In our study, for each model, we perform a set of solar cycle simulations at $\hat{\alpha}_0 = 2, 4$, and 8 , and for each model, the level of fluctuations in α remains the same.

From each model, we compute several properties, namely, the recovery rate from Maunder-like grand minimum, the number and duration of grand minimum and maximum, the correlation between the polar field at cycle minimum with the amplitude of the next cycle toroidal field, and the Gnevyshev–Ohl/Even–Odd Rule. Below, we discuss their results.

3.1. Recovery Rate of Maunder Minimum

We know that during Maunder minimum, the Sun went to a deep minimum of magnetic activity for at least 40 years (Eddy, 1976; Ribes and Nesme-Ribes, 1993; Usoskin, 2023). While the triggering phase of the Maunder minimum is somewhat uncertain, its recovery phase is a bit gradual. During about 1700 to 1730, the Sun gradually recovered from the quiet phase to the normal one. Although we have these details for only one grand minimum, we can use this rate of recovery from the Maunder minimum to learn about the dynamo growth

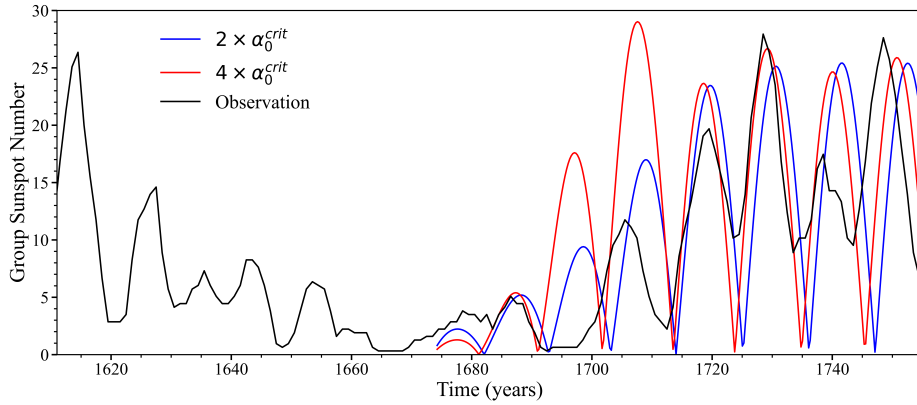


Figure 1. The plot depicting the comparison of recovery rates from Maunder minimum. The black line is the observational data of Maunder minimum (yearly mean group sunspot number available during 1610–2015 obtained from WDC-SILSO, Royal Observatory of Belgium, Brussels). The blue and red lines represent the model data at $\hat{\alpha}_0 = 2$, and $\hat{\alpha}_0 = 4$ from Model I.

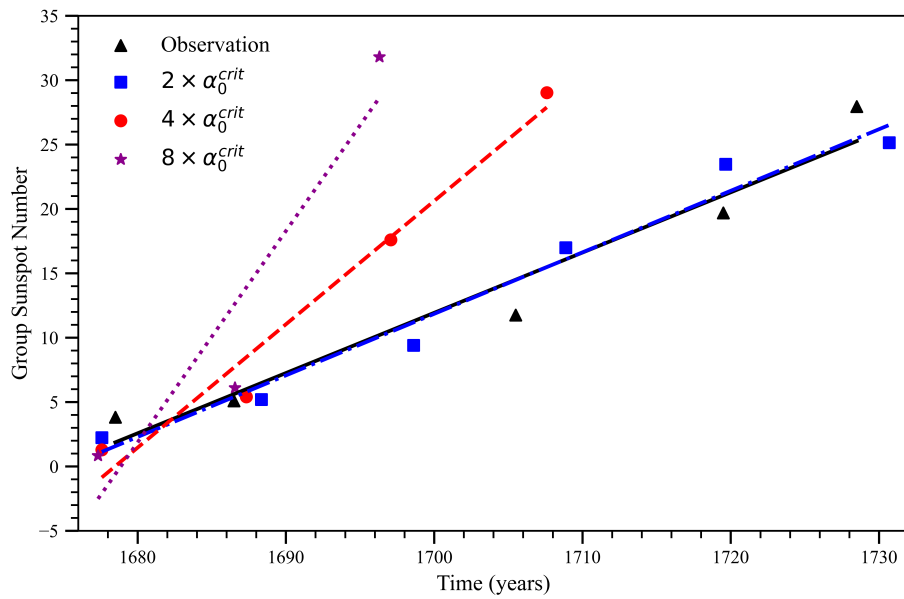


Figure 2. The plot compares the recovery rates from the Maunder Minimum. Black/triangles show the observed recovery rate, and blue/squares, red/circles, and dark magenta/asterisks (and connecting lines) represent model recovery rates at $\hat{\alpha}_0 = 2$, 4, and 8 respectively in Model I.

rate, which is related to the supercriticality of the Sun. To do so, we manually cut the magnetic field in the dynamo model by multiplying the poloidal field at the solar minimum by a factor of $\gamma_p = 0.1$. We note that this idea was based on the work of Choudhuri and Karak (2009), who proposed that due to fluctuations in the Babcock-Leighton process, the polar field at the solar minimum can be largely different, and to capture this in their model, they multiplied the polar field at the solar minimum by a factor γ_p . After multiplying the polar field at the solar minimum by a factor of γ_p , we run the model for several cycles to examine its recovery to the normal phase at different values of $\hat{\alpha}_0$.

Figure 1 shows the recovery of the model from the Maunder minimum in Models I at $\hat{\alpha}_0 = 2$ and 4 (blue and red curves) and their comparison with the observed data (black curve).

To make a better comparison of the observed peaks of the cycles during the recovery phase of the Maunder minimum with the model, in Figure 2 we present the slopes of the observed data from the Maunder minimum (black curve) and from the model (blue, red and dark magenta) at $\hat{\alpha}_0 = 2, 4$ and 8. We see that as $\hat{\alpha}_0$ is increased, the model deviates more and more from the observed one. We have repeated this exercise using other models and find consistent results in Models II, III and IV. The Model V is however excluded in this study because this model produces chaotic solution and the recovery rate is quite different even at a slight different value of α_0 .

The reason for the robust result in all four models (I–VI) is not difficult to understand. As $\hat{\alpha}_0$ increases, the dynamo becomes stronger (dynamo number increases), and it allows the magnetic field to grow more rapidly. In summary, from the analysis of the recovery rate of Maunder minimum, we can expect that the supercriticality of the sun as measured by $\hat{\alpha}_0$ is around two.

3.2. Statistics of Grand Minima and Maxima

Next, we compute the grand minima and maxima frequency using different models with varying supercriticality. To produce grand minima and maxima in our kinematic dynamo, we follow the traditional methods, i.e., we include fluctuations in the poloidal source to mimic the variations in the flux emergence and BMR properties (Karak, 2023). Explicitly, we include stochastic fluctuations in the amplitude of the α (both in Babcock–Leighton and mean-field) as mentioned in the Section 2. The details of the level of fluctuations and the coherence time in each model are mentioned in the first column of Table 1 (also see model section). By running five models at different values of $\hat{\alpha}_0$, each for 11,000 years (the same duration for which the reconstructed solar activity is available; Usoskin (2023)), we compute the statistics of grand minima and maxima. To compute the grand minima/maxima, we follow the same procedure as used in the observational study of Usoskin, Solanki, and Kovaltsov (2007). We first bin the toroidal flux data computed at the base of CZ at low latitude ($r = 0.72R_\odot$, $\theta = 10^\circ$ to 45°) using a window of the length of the average cycle duration and then smoothing the binned data using Gleissberg’s low-pass filter 1-2-2-2-1. The time series of these data is shown in Figure 3 for $\hat{\alpha}_0 = 2$ and 4 from Model I. Finally, we define an episode as a grand minimum (maximum)

Table 1. The number of grand minima and maxima obtained from 11,000 years of simulations using different models at different dynamo supercriticality as measured by $\hat{\alpha}_0$. The critical value for the Babcock–Leighton α in each model is given in the second column.

Models ($\hat{\alpha}_0$)	α_0^{crit} (m s ⁻¹)	Grand Minima			Grand Maxima		
		2.0	4.0	8.0	2.0	4.0	8.0
Model I Kumar, Karak, and Vashishth (2021) ($\sigma = 2.67$ Gaussian fluctuation)	0.38 (m s ⁻¹)	20	8	5	22	16	18
Model II Kumar, Karak, and Vashishth (2021) ($\sigma = 2.67$ Gaussian fluctuations)	0.05 (m s ⁻¹)	18	8	6	22	15	13
Model III Passos et al. (2014) (200% uniform fluctuations)	18.9 (m s ⁻¹)	16	9	4	26	8	3
Model IV Hazra, Passos, and Nandy (2014) (100% uniform fluctuations)	0.16	26	11	10	27	21	21
Model V Albert et al. (2021) (70% uniform fluctuations)	10.2	20	16	9	24	14	9
Observed		27			23		

when this smoothed data remains below (or above) 50% (150%) of the average of the whole time series for at least two-cycle duration continuously; see blue and red shaded regions for grand minima and maxima in Figure 3. As shown in Table 1, at $\hat{\alpha}_0 = 2$, the numbers of grand minima in Model I and II are 20 and 18, respectively, and as the value of $\hat{\alpha}_0$ is increased, the number decreases. A similar result is seen for grand maxima, although the decrease is not monotonous. To explore the robustness of these trends of grand minima/maxima with the $\hat{\alpha}_0$, we repeat these studies using other models, namely, Models III–VI. We find similar trends in these models as well; see Table 1. We recall that from the cosmogenic isotope records of Usoskin, Solanki, and Kovaltsov (2007), we know that Sun produced 27 grand minima and 23 grand maxima in the last 11,000 years. Thus, it suggests that the models at $\hat{\alpha}_0 = 2$ are closer to observations, implying that the solar dynamo is operating near the critical regime of the dynamo and far from the supercritical regime. Our result also agrees with the previous suggestions that the grand minima are more frequent in weakly supercritical dynamo (Karak and Choudhuri, 2013; Olemskoy and Kitchatinov, 2013).

Further analysing the properties of grand minima/maxima, we find that the percentage of time spent in grand minima decreases and the duration of grand minima becomes shorter with the increase of the supercriticality of the dynamo (Figure 4 and Table 2). The long duration grand minima (Spörer-like) are not

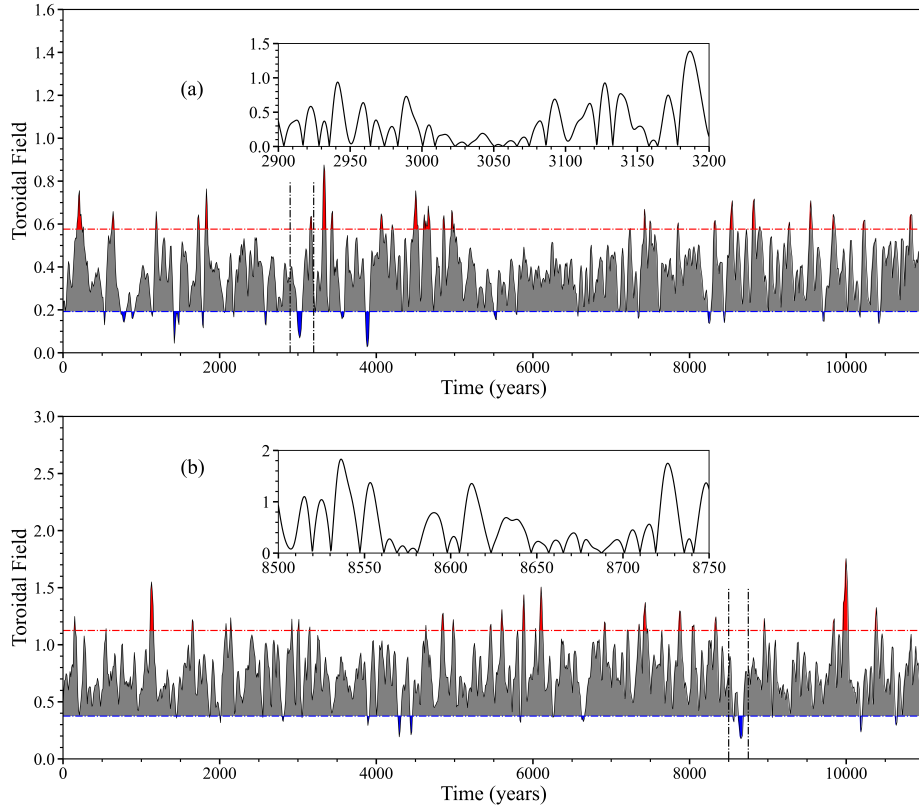


Figure 3. Temporal variation of the smoothed toroidal field of 11,000-year simulation of Model I. Blue-shaded regions below the horizontal blue line represent the grand minima, whereas red-shaded regions above the horizontal red line represent the grand maxima; (a) for $\hat{\alpha}_0 = 2$, and (b) for $\hat{\alpha}_0 = 4$. Insets show epochs around a grand minimum

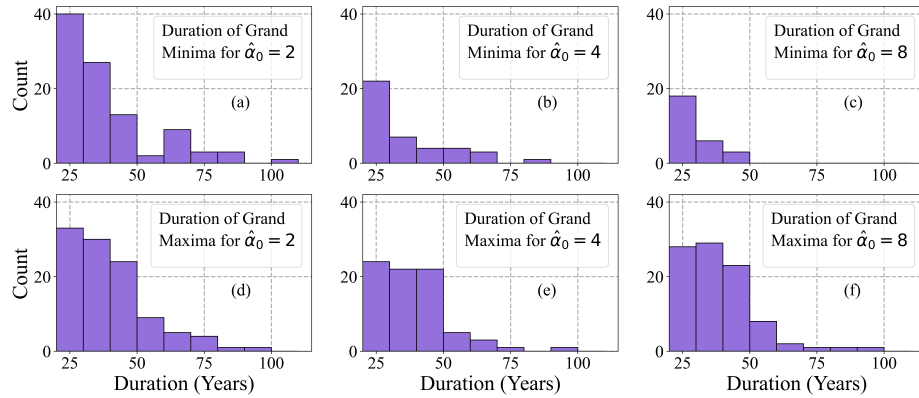


Figure 4. Histograms for the durations of grand minima (a,b,c) and grand maxima (d, e, f) with increasing dynamo supercriticality ($\hat{\alpha}_0$).

Table 2. Percentage of time spent in grand minima and maxima obtained for different values of $\hat{\alpha}_0$. The values in parentheses are the average duration of grand minima and maxima in years. For the time delay models, the time is in a dimensionless unit and thus not shown.

Models ($\hat{\alpha}_0$)	Minima			Maxima		
	2.0	4.0	8.0	2.0	4.0	8.0
Model I Kumar, Karak, and Vashishth (2021) ($\sigma = 2.67$ Gaussian fluctuation)	6.0 (33.9)	2.3 (31)	1.2 (24.4)	6.8 (34.8)	4.8 (33.5)	5.7 (33.4)
Model II Kumar, Karak, and Vashishth (2021) ($\sigma = 2.67$ Gaussian fluctuation)	4.3 (29.6)	1.8 (26.6)	1.7 (31.3)	7.2 (36.6)	4.8 (33.9)	4.0 (33)
Model III Passos et al. (2014) (200% fluctuation)	13.4 (92.1)	3.4 (41.1)	0.8 (22.5)	13.2 (55.8)	2.3 (31.3)	0.74 (27)
Model IV Hazra, Passos, and Nandy (2014) (100% fluctuation)	5.4	0.4	0.4	4.9	0.9	0.6
Model V Albert et al. (2021) (70% fluctuation)	22.5	30.0	7.5	41.7	22.3	10.5

seen at $\hat{\alpha}_0 = 4$. Even the Maunder-like grand minima are not detected at $\hat{\alpha}_0 = 8$; Figure 4c. For the grand maxima, surprisingly, we do not observe much change in the duration. In all models considered in our study, we observe similar behaviour as demonstrated by the change of the average duration of grand minima/maxima with $\hat{\alpha}_0$. Again, from the average duration of grand minima and maxima at different $\hat{\alpha}_0$ (Table 2 and Figure 4), we conclude that the $\hat{\alpha}_0 = 2$ is more favorable for the solar dynamo.

3.3. Do the features of solar cycle at two times critical dynamo contradict with observations?

3.3.1. Correlation between the polar field and the sunspot cycle

In any $\alpha \Omega$ dynamo model, as long as the poloidal field acts as the source for the toroidal field, there exists a strong correlation between the poloidal (or polar) field at the cycle minimum and the toroidal field of the next cycle (Charbonneau and Barlet, 2011). Now the question is whether this memory of the poloidal field is propagated beyond one cycle toroidal field. Kumar, Karak, and Vashishth (2021) showed that the answer depends on the supercriticality of the dynamo. When the dynamo operates near critical dynamo transition, both the magnetic field growth rate and the nonlinearity are weak, which supports multi cycle memory of the polar field. On the other hand, when the dynamo is highly supercritical, the growth rate of the magnetic field is high, and the nonlinearity is also

Table 3. Comparison of the Pearson correlation coefficient between the polar flux (or its proxy) of cycle n and toroidal flux (or sunspot area) of cycles n , $n + 1$, $n + 2$, and $n + 3$ from Models I and II, and observation. The values from models are obtained from Kumar, Karak, and Vashishth (2021) at 2 times critical ($\hat{\alpha}_0 = 2$), while the observed values are taken from Muñoz-Jaramillo et al. (2013).

$\phi_r(n)$ &	Model I	Model II	Observations
$\phi_{tor}(n)$	-0.07	0.19	0.16
$\phi_{tor}(n + 1)$	0.99	0.97	0.60
$\phi_{tor}(n + 2)$	-0.09	0.29	0.27
$\phi_{tor}(n + 3)$	0.18	0.20	-0.23

efficient, which tries to break the memory of the magnetic field. By performing stochastically forced dynamo simulations at different parameter regimes and varying prescriptions for the poloidal sources, Kumar, Karak, and Vashishth (2021) demonstrated that the memory of the poloidal field is propagated to multiple cycles when the dynamo operates near the critical dynamo transition. However, if the dynamo is highly supercritical, then the memory of the polar field is limited to only the next cycle toroidal field (also see Ghosh et al., 2024, for supporting this result using an independent study).

Our present study favours $\hat{\alpha}_0 = 2$ for the Sun, which implies that the solar dynamo is neither critical nor heavily supercritical. Thus, following Kumar, Karak, and Vashishth (2021) study, we expect a negligible correlation between the polar field at the end of cycle n with the toroidal field for cycle $n + 2$ and $n + 3$; see Table 3 from Kumar, Karak, and Vashishth (2021)). On the other hand, analysing the polar faculae counts—a proxy of the polar field—Muñoz-Jaramillo et al. (2013) showed that there is no significant correlation between the polar field (faculae count) of cycle n with the toroidal field (sunspot area) of cycles $n + 2$ and $n + 3$; see the last column of Table 3. Hence, the conclusion that the Sun is about two times supercritical does not contradict the observed data.

We want to add that the observed correlation, as reported by Muñoz-Jaramillo et al. (2013), is based on a limited number of data (10 cycles or 20 data points by separating hemispheres). And we can observe from Figure 5, that the $n + 2$ and $n + 3$ (weak) correlations are highly fluctuating when the data point is below about 100. Hence, the observed no correlation beyond $n + 1$ does not utterly confirm that the polar field of the Sun does not have memory beyond one cycle and that the Sun’s super-criticality is precisely two times. Nevertheless, the available data does not contradict the conclusion that is drawn in the previous section about the Sun’s supercriticality.

3.3.2. Gnevyshev–Ohl/Even–Odd Rule

Finally, we shall check another feature of the solar cycle at two times critical dynamo models, and that is Gnevyshev–Ohl, also called the even-odd rule (Hathaway, 2015; Karak, 2023). This rule says that if the cycles are arranged in pairs

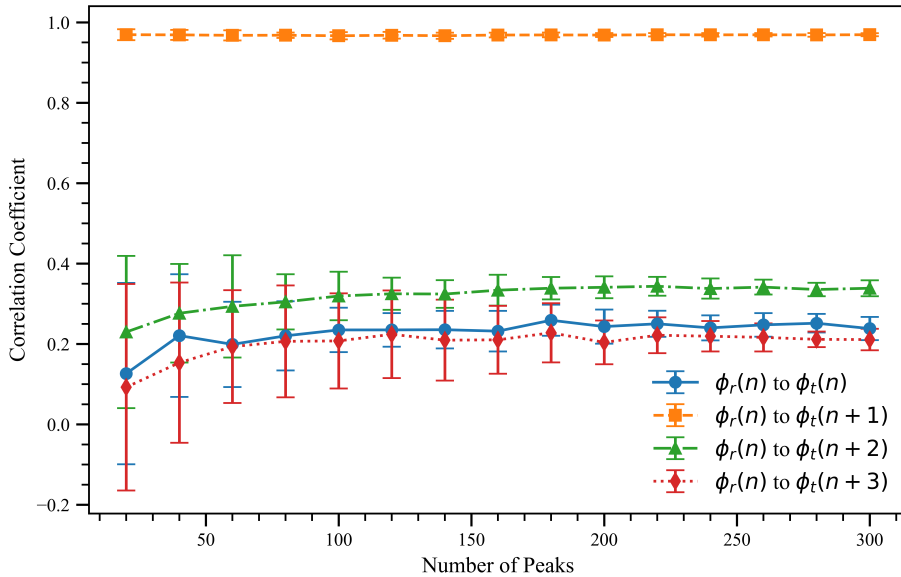


Figure 5. Pearson Correlation coefficients between the polar flux at cycle n with the toroidal flux at cycle $n+1$ (blue/filled-circles), $n+2$ (red/squares), and $n+3$ (black/triangles) computed for a different number of cycles from Model II at $\hat{\alpha}_0 = 2$. The points show the average values computed from 20 data sets, and the error bar shows the standard deviation.

with the even cycle and the following odd cycle, then the sum of the sunspot number in the odd cycle would be higher than the even one. Out of the last 24 solar cycles, this law did not apply for 4-5 and 22-23 pairs (Hathaway, 2015). We check whether our dynamo models at two times supercritical demonstrate this feature. To do so, we compute the probability distribution function (PDF) of the length of the even-odd pair, which is shown by the blue line in Figure 6. As for this analysis, we need longer data; we preferred to demonstrate this for the time delay model (Model IV), which is computationally cheap. To compare with the observed data, we have computed PDF from the observed sunspot number of the last ten cycles in conjunction with the reconstructed sunspot number of the last millennium from Usoskin et al. (2021), which is shown by the solid black line in Figure 6. We note that excluding the grand minima phases, we got data points of only seventy-two cycles during normal phases. Using the errors in the reconstructed sunspot number as reported in Usoskin et al. (2022), we generated 1σ errors in the PDF. Although the PDF computed from the observed data is not robust due to the limited number of data and a huge uncertainty in the reconstruction (Usoskin, 2023), we can say that the model PDF at two times supercritical is not in contradiction to the observed data.

4. Conclusions

With the increase of age, the dynamo activity of stars decreases due to the weakening of the rotation rate and, thus, the magnetic field generation efficiency

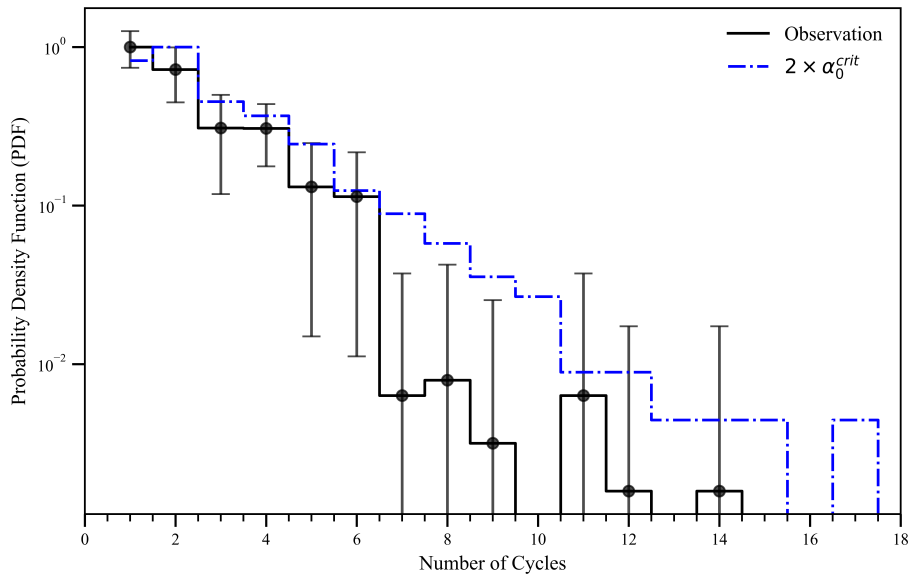


Figure 6. PDF of the duration of the even-odd episodes measured at different values of $\hat{\alpha}_0$ from Model IV (time delay dynamo model). The observation PDF is computed using the last 10 cycles sunspot data and the reconstructed sunspot number of Usoskin et al. (2021) with error from Usoskin et al. (2022), excluding the grand minima episodes.

of the dynamo. At some point, stars are expected to reach the subcritical regimes when the dynamo will cease to generate a large-scale magnetic field. We tried to explore how far our Sun is from the critical dynamo transition, in other words, how supercritical our solar dynamo is. To answer this question, we have executed extensive dynamo simulations at different values of the α coefficient as measured by $\hat{\alpha}_0 = \alpha_0/\alpha_0^{\text{crit}}$. By comparing various features of magnetic cycles, namely, the statistics of grand minima/maxima and the recovery rate of Maunder minimum, we conclude that the supercriticality of the solar dynamo is only about two times the critical dynamo ($\hat{\alpha}_0 = 2$). We also showed that this two-times critical dynamo does not contradict the observed correlations between the polar field vs the amplitude of the following cycles as presented in Muñoz-Jaramillo et al. (2013) and the probability of the even-odd pairing rule. While we have presented our conclusion based on several dynamo models, all are kinematic in nature, and the nonlinearity is specified. However, our conclusion is in line with previous independent studies, which also hint at the weakly supercriticality of the solar dynamo (Kitchatinov and Nepomnyashchikh, 2017; Cameron and Schüssler, 2017, 2019; Ghosh et al., 2024).

5. Acknowledgements

The authors gratefully acknowledge the constructive comments and suggestions from the anonymous referee. The authors also thank Vindya Vashishth and

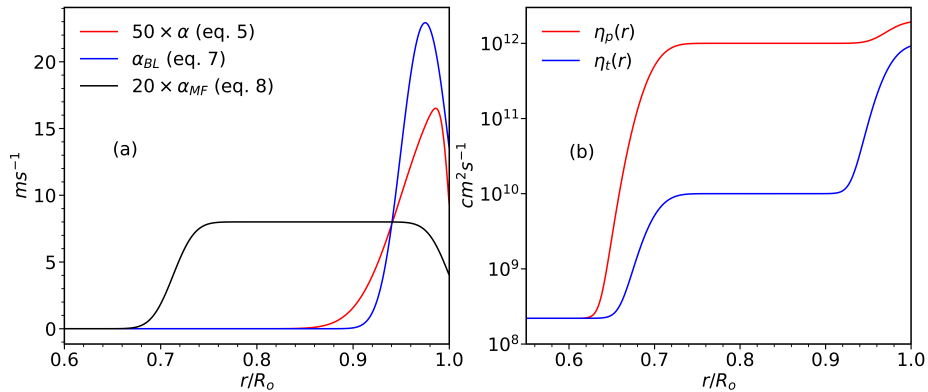


Figure 7. (a): Red and blue curves show the α profile for non-local (for Models I and II), and local (Model III) prescription of Babcock–Leighton process. The black curve represents the mean-field α profile for Model III, as discussed in Section 2.1. (b) Variations of η_p (red) and η_t (blue) used in Model III.

Dipanwita Mishra for their valuable comments and discussions. The authors acknowledge the Science and Engineering Research Board (SERB) for providing financial support through the MATRIC program (file no. MTR/2023/000670).

6. Data Availability

We have used the SSN data available at SILSO (www.sidc.be/SILSO/datafiles). Polar field data is taken from Wilcox Solar Observatory (WSO) (<http://wso.stanford.edu/Polar.html>).

7. Appendix

In this study, we have used different models which use different profiles of α , η , and the quenching. We have already discussed these parameters in the model section in detail. Here, we demonstrate the profiles of different dynamo parameters using Figures 7 and 8.

References

- Albert, C., Ferriz-Mas, A., Gaia, F., Ulzega, S.: 2021, Can Stochastic Resonance Explain Recurrence of Grand Minima? *Astrophys. J. Lett.* **916**, L9. [DOI](#). [ADS](#).
- Augustson, K., Brun, A.S., Miesch, M., Toomre, J.: 2015, Grand Minima and Equatorward Propagation in a Cycling Stellar Convective Dynamo. *Astrophys. J.* **809**, 149. [DOI](#). [ADS](#).
- Babcock, H.W.: 1961, The Topology of the Sun’s Magnetic Field and the 22-YEAR Cycle. *Astrophys. J.* **133**, 572. [DOI](#). [ADS](#).
- Bhowmik, P., Nandy, D.: 2018, Prediction of the strength and timing of sunspot cycle 25 reveal decadal-scale space environmental conditions. *Nature Communications* **9**, 5209. [DOI](#). [ADS](#).
- Biswas, A., Karak, B.B., Kumar, P.: 2023, Exploring the reliability of polar field rise rate as a precursor for an early prediction of solar cycle. *Mon. Not. R. Astron. Soc.* **526**, 3994. [DOI](#). [ADS](#).

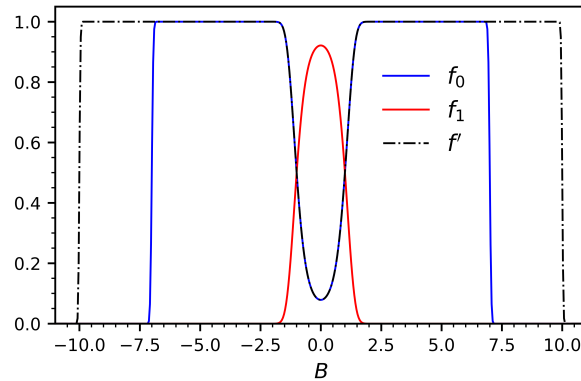


Figure 8. Profiles of the α quenching function used in Models IV and V. Functions f_0 and f_1 correspond to Babcock–Leighton α (blue) and mean field α (red) used in Model IV. The quenching f' corresponds to Babcock–Leighton α in Model V is shown in black.

- Biswas, A., Karak, B.B., Usoskin, I., Weisshaar, E.: 2023, Long-Term Modulation of Solar Cycles. *Space Sci. Rev.* **219**, 19. DOI. ADS.
- Brun, A.S., Browning, M.K.: 2017, Magnetism, dynamo action and the solar-stellar connection. *Living Reviews in Solar Physics* **14**, 4. DOI. ADS.
- Brun, A.S., Miesch, M.S., Toomre, J.: 2004, Global-Scale Turbulent Convection and Magnetic Dynamo Action in the Solar Envelope. *Astrophys. J.* **614**, 1073. DOI. ADS.
- Brun, A.S., Strugarek, A., Varela, J., Matt, S.P., Augustson, K.C., Emeriau, C., DoCao, O.L., Brown, B., Toomre, J.: 2017, On Differential Rotation and Overshooting in Solar-like Stars. *Astrophys. J.* **836**, 192. DOI. ADS.
- Brun, A.S., Strugarek, A., Noraz, Q., Perri, B., Varela, J., Augustson, K., Charbonneau, P., Toomre, J.: 2022, Powering Stellar Magnetism: Energy Transfers in Cyclic Dynamos of Sun-like Stars. *Astrophys. J.* **926**, 21. DOI. ADS.
- Cameron, R., Schüssler, M.: 2015, The crucial role of surface magnetic fields for the solar dynamo. *Science* **347**, 1333. DOI. ADS.
- Cameron, R.H., Schüssler, M.: 2017, Understanding Solar Cycle Variability. *Astrophys. J.* **843**, 111. DOI. ADS.
- Cameron, R.H., Schüssler, M.: 2019, Solar activity: periodicities beyond 11 years are consistent with random forcing. *Astron. Astrophys.* **625**, A28. DOI. ADS.
- Cameron, R.H., Schüssler, M.: 2023, Observationally Guided Models for the Solar Dynamo and the Role of the Surface Field. *Space Sci. Rev.* **219**, 60. DOI. ADS.
- Charbonneau, P.: 2020, Dynamo models of the solar cycle. *Living Reviews in Solar Physics* **17**, 4. DOI. ADS.
- Charbonneau, P., Barlet, G.: 2011, The dynamo basis of solar cycle precursor schemes. *Journal of Atmospheric and Solar-Terrestrial Physics* **73**, 198. DOI. ADS.
- Charbonneau, P., Dikpati, M.: 2000, Stochastic Fluctuations in a Babcock–Leighton Model of the Solar Cycle. *Astrophys. J.* **543**, 1027. DOI. ADS.
- Charbonneau, P., Blais-Laurier, G., St-Jean, C.: 2004, Intermittency and Phase Persistence in a Babcock–Leighton Model of the Solar Cycle. *Astrophys. J. Lett.* **616**, L183. DOI. ADS.
- Charbonneau, P., St-Jean, C., Zacharias, P.: 2005, Fluctuations in Babcock–Leighton Dynamos. I. Period Doubling and Transition to Chaos. *Astrophys. J.* **619**, 613. DOI. ADS.
- Chatterjee, P., Nandy, D., Choudhuri, A.R.: 2004, Full-sphere simulations of a circulation-dominated solar dynamo: Exploring the parity issue. *Astron. Astrophys.* **427**, 1019. DOI. ADS.
- Choudhuri, A.R., Hazra, G.: 2016, The treatment of magnetic buoyancy in flux transport dynamo models. *Advances in Space Research* **58**, 1560. DOI. ADS.
- Choudhuri, A.R., Karak, B.B.: 2009, A possible explanation of the Maunder minimum from a flux transport dynamo model. *Res. Astron. Astrophys.* **9**, 953. DOI. ADS.
- Choudhuri, A.R., Karak, B.B.: 2012, Origin of Grand Minima in Sunspot Cycles. *Phys. Rev. Lett.* **109**, 171103.

- Choudhuri, A.R., Chatterjee, P., Jiang, J.: 2007, Predicting Solar Cycle 24 With a Solar Dynamo Model. *Physical Review Letters* **98**, 131103. DOI. ADS.
- Choudhuri, A.R., Nandy, D., Chatterjee, P.: 2005, Reply to the Comments of Dikpati et al. *Astron. Astrophys.* **437**, 703. DOI. ADS.
- Choudhuri, A.R., Schüssler, M., Dikpati, M.: 1995, The solar dynamo with meridional circulation. *Astron. Astrophys.* **303**, L29. ADS.
- Dasi-Espuig, M., Solanki, S.K., Krivova, N.A., Cameron, R., Peñuela, T.: 2010, Sunspot group tilt angles and the strength of the solar cycle. *Astron. Astrophys.* **518**, A7. DOI. ADS.
- Dikpati, M., Charbonneau, P.: 1999, A Babcock-Leighton Flux Transport Dynamo with Solar-like Differential Rotation. *Astrophys. J.* **518**, 508. DOI. ADS.
- Eddy, J.A.: 1976, The Maunder Minimum. *Science* **192**, 1189. DOI. ADS.
- Fan, Y., Fang, F.: 2014, A Simulation of Convective Dynamo in the Solar Convective Envelope: Maintenance of the Solar-like Differential Rotation and Emerging Flux. *Astrophys. J.* **789**, 35. DOI. ADS.
- Garg, S., Karak, B.B., Egeland, R., Soon, W., Baliunas, S.: 2019, Waldmeier Effect in Stellar Cycles. *arXiv e-prints*, arXiv:1909.12148. ADS.
- Ghosh, A., Kumar, P., Prasad, A., Karak, B.B.: 2024, Characterizing the Solar Cycle Variability Using Nonlinear Time Series Analysis at Different Amounts of Dynamo Supercriticality: Solar Dynamo is Not Highly Supercritical. *Astron. J.* **167**, 209. DOI. ADS.
- Hathaway, D.H.: 2015, The Solar Cycle. *Living Reviews in Solar Physics* **12**, 4. DOI. ADS.
- Hazra, G., Choudhuri, A.R.: 2019, A New Formula for Predicting Solar Cycles. *Astrophys. J.* **880**, 113. DOI. ADS.
- Hazra, G., Nandy, D., Kitchatinov, L., Choudhuri, A.R.: 2023, Mean Field Models of Flux Transport Dynamo and Meridional Circulation in the Sun and Stars. *Space Sci. Rev.* **219**, 39. DOI. ADS.
- Hazra, S., Passos, D., Nandy, D.: 2014, A Stochastically Forced Time Delay Solar Dynamo Model: Self-consistent Recovery from a Maunder-like Grand Minimum Necessitates a Mean-field Alpha Effect. *Astrophys. J.* **789**, 5. DOI. ADS.
- Hotta, H., Kusano, K., Shimada, R.: 2022, Generation of Solar-like Differential Rotation. *Astrophys. J.* **933**, 199. DOI. ADS.
- Jha, B.K., Karak, B.B., Mandal, S., Banerjee, D.: 2020, Magnetic Field Dependence of Bipolar Magnetic Region Tilts on the Sun: Indication of Tilt Quenching. *Astrophys. J. Lett.* **889**, L19. DOI. ADS.
- Jiang, J., Cameron, R.H., Schüssler, M.: 2014, Effects of the Scatter in Sunspot Group Tilt Angles on the Large-scale Magnetic Field at the Solar Surface. *Astrophys. J.* **791**, 5. DOI. ADS.
- Käpylä, M.J., Käpylä, P.J., Olsper, N., Brandenburg, A., Warnecke, J., Karak, B.B., Pelt, J.: 2016, Multiple dynamo modes as a mechanism for long-term solar activity variations. *Astron. Astrophys.* **589**, A56. DOI. ADS.
- Käpylä, P.J., Browning, M.K., Brun, A.S., Guerrero, G., Warnecke, J.: 2023, Simulations of Solar and Stellar Dynamos and Their Theoretical Interpretation. *Space Sci. Rev.* **219**, 58. DOI. ADS.
- Karak, B.B.: 2010, Importance of Meridional Circulation in Flux Transport Dynamo: The Possibility of a Maunder-like Grand Minimum. *Astrophys. J.* **724**, 1021. DOI. ADS.
- Karak, B.B.: 2023, Models for the long-term variations of solar activity. *Living Reviews in Solar Physics* **20**, 3. DOI. ADS.
- Karak, B.B., Choudhuri, A.R.: 2013, Studies of grand minima in sunspot cycles by using a flux transport solar dynamo model. *Res. Astron. Astrophys.* **13**, 1339. DOI. ADS.
- Karak, B.B., Miesch, M.: 2017, Solar Cycle Variability Induced by Tilt Angle Scatter in a Babcock-Leighton Solar Dynamo Model. *Astrophys. J.* **847**, 69. DOI. ADS.
- Karak, B.B., Miesch, M.: 2018, Recovery from Maunder-like Grand Minima in a Babcock-Leighton Solar Dynamo Model. *Astrophys. J. Lett.* **860**, L26. DOI. ADS.
- Karak, B.B., Kitchatinov, L.L., Brandenburg, A.: 2015, Hysteresis between Distinct Modes of Turbulent Dynamos. *Astrophys. J.* **803**, 95. DOI. ADS.
- Karak, B.B., Mandal, S., Banerjee, D.: 2018, Double Peaks of the Solar Cycle: An Explanation from a Dynamo Model. *Astrophys. J.* **866**, 17. DOI. ADS.
- Karak, B.B., Miesch, M., Bekki, Y.: 2018, Consequences of high effective Prandtl number on solar differential rotation and convective velocity. *Physics of Fluids* **30**, 046602. DOI. ADS.
- Karak, B.B., Jiang, J., Miesch, M.S., Charbonneau, P., Choudhuri, A.R.: 2014, Flux Transport Dynamos: From Kinematics to Dynamics. *Space Sci. Rev.* **186**, 561. DOI. ADS.

- Karak, B.B., Käpylä, P.J., Käpylä, M.J., Brandenburg, A., Olsper, N., Pelt, J.: 2015, Magnetically controlled stellar differential rotation near the transition from solar to anti-solar profiles. *Astron. Astrophys.* **576**, A26. DOI ADS.
- Kitchatinov, L., Nepomnyashchikh, A.: 2017, How supercritical are stellar dynamos, or why do old main-sequence dwarfs not obey gyrochronology? *Mon. Not. R. Astron. Soc.* **470**, 3124. DOI ADS.
- Kitchatinov, L.L., Olemskoy, S.V.: 2010, Dynamo hysteresis and grand minima of solar activity. *Astron. Lett.* **36**, 292.
- Kitchatinov, L.L., Olemskoy, S.V.: 2011, Does the Babcock-Leighton mechanism operate on the Sun? *Astronomy Letters* **37**, 656. DOI ADS.
- Krause, F., Rädler, K.H.: 1980, *Mean-field magnetohydrodynamics and dynamo theory*, Oxford: Pergamon Press.
- Kumar, P., Biswas, A., Karak, B.B.: 2022, Physical link of the polar field buildup with the Waldmeier effect broadens the scope of early solar cycle prediction: Cycle 25 is likely to be slightly stronger than Cycle 24. *Mon. Not. R. Astron. Soc.* **513**, L112. DOI ADS.
- Kumar, P., Karak, B.B., Sreedevi, A.: 2024, Variabilities in the polar field and solar cycle due to irregular properties of Bipolar Magnetic Regions. *Mon. Not. R. Astron. Soc.* DOI ADS.
- Kumar, P., Karak, B.B., Vashishth, V.: 2021, Supercriticality of the Dynamo Limits the Memory of the Polar Field to One Cycle. *Astrophys. J.* **913**, 65. DOI ADS.
- Kumar, P., Nagy, M., Lemerle, A., Karak, B.B., Petrovay, K.: 2021, The Polar Precursor Method for Solar Cycle Prediction: Comparison of Predictors and Their Temporal Range. *Astrophys. J.* **909**, 87. DOI ADS.
- Leighton, R.B.: 1969, A Magneto-Kinematic Model of the Solar Cycle. *Astrophys. J.* **156**, 1. DOI ADS.
- Metcalfe, T.S., Egeland, R., van Saders, J.: 2016, Stellar Evidence That the Solar Dynamo May Be in Transition. *Astrophys. J. Lett.* **826**, L2. DOI ADS.
- Moffatt, H.K.: 1978, *Magnetic field generation in electrically conducting fluids*. ADS.
- Mordvinov, A.V., Karak, B.B., Banerjee, D., Golubeva, E.M., Khlystova, A.I., Zhukova, A.V., Kumar, P.: 2022, Evolution of the Sun's activity and the poleward transport of remnant magnetic flux in Cycles 21-24. *Mon. Not. R. Astron. Soc.* **510**, 1331. DOI ADS.
- Muñoz-Jaramillo, A., Dasi-Espuig, M., Balmaceda, L.A., DeLuca, E.E.: 2013, Solar Cycle Propagation, Memory, and Prediction: Insights from a Century of Magnetic Proxies. *Astrophys. J. Lett.* **767**, L25. DOI ADS.
- Noyes, R.W., Hartmann, L.W., Baliunas, S.L., Duncan, D.K., Vaughan, A.H.: 1984, Rotation, convection, and magnetic activity in lower main-sequence stars. *Astrophys. J.* **279**, 763. DOI ADS.
- Olemskoy, S.V., Kitchatinov, L.L.: 2013, Grand Minima and North-South Asymmetry of Solar Activity. *Astrophys. J.* **777**, 71.
- Olemskoy, S.V., Choudhuri, A.R., Kitchatinov, L.L.: 2013, Fluctuations in the alpha-effect and grand solar minima. *Astronomy Reports* **57**, 458. DOI ADS.
- Parker, E.N.: 1955, Hydromagnetic Dynamo Models. *Astrophys. J.* **122**, 293. DOI ADS.
- Passos, D., Nandy, D., Hazra, S., Lopes, I.: 2014, A solar dynamo model driven by mean-field alpha and Babcock-Leighton sources: fluctuations, grand-minima-maxima, and hemispheric asymmetry in sunspot cycles. *Astron. Astrophys.* **563**, A18. DOI ADS.
- Racine, É., Charbonneau, P., Ghizaru, M., Bouchat, A., Smolarkiewicz, P.K.: 2011, On the Mode of Dynamo Action in a Global Large-eddy Simulation of Solar Convection. *Astrophys. J.* **735**, 46. DOI ADS.
- Rengarajan, T.N.: 1984, Age-rotation relationship for late-type main-sequence stars. *Astrophys. J. Lett.* **283**, L63.
- Ribes, J.C., Nesme-Ribes, E.: 1993, The solar sunspot cycle in the Maunder minimum AD1645 to AD1715. *Astron. Astrophys.* **276**, 549. ADS.
- Schatten, K.H., Scherrer, P.H., Svalgaard, L., Wilcox, J.M.: 1978, Using dynamo theory to predict the sunspot number during solar cycle 21. *Geophys. Res. Lett.* **5**, 411. DOI ADS.
- Shah, S.P., Wright, J.T., Isaacson, H., Howard, A.W., Curtis, J.L.: 2018, HD 4915: A Maunder Minimum Candidate. *Astrophys. J. Lett.* **863**, L26. DOI ADS.
- Skumanich, A.: 1972, Time Scales for CA II Emission Decay, Rotational Braking, and Lithium Depletion. *Astrophys. J.* **171**, 565. DOI ADS.
- Sreedevi, A., Jha, B.K., Karak, B.B., Banerjee, D.: 2024, Analysis of BMR Tilt from AutoTAB Catalog: Hinting toward the Thin Flux Tube Model? *Astrophys. J.* **966**, 112. DOI ADS.
- Strugarek, A., Beaudoin, P., Charbonneau, P., Brun, A.S.: 2018, On the Sensitivity of Magnetic Cycles in Global Simulations of Solar-like Stars. *Astrophys. J.* **863**, 35. DOI ADS.

- Tripathi, B., Nandy, D., Banerjee, S.: 2021, Stellar mid-life crisis: subcritical magnetic dynamos of solar-like stars and the breakdown of gyrochronology. *Mon. Not. R. Astron. Soc.* **506**, L50. DOI. ADS.
- Usoskin, I.G.: 2023, A history of solar activity over millennia. *Living Reviews in Solar Physics* **20**, 2. DOI. ADS.
- Usoskin, I.G., Solanki, S.K., Kovaltsov, G.A.: 2007, Grand minima and maxima of solar activity: new observational constraints. *Astron. Astrophys.* **471**, 301.
- Usoskin, I.G., Solanki, S.K., Krivova, N.A., Hofer, B., Kovaltsov, G.A., Wacker, L., Brehm, N., Kromer, B.: 2021, Solar cyclic activity over the last millennium reconstructed from annual ^{14}C data. *Astron. Astrophys.* **649**, A141. DOI. ADS.
- Usoskin, I.G., Solanki, S.K., Krivova, N., Hofer, B., Kovaltsov, G.A., Wacker, L., Brehm, N., Kromer, B.: 2022, Solar cyclic activity over the last millennium reconstructed from annual ^{14}C data (Corrigendum). *Astron. Astrophys.* **664**, C3. DOI. ADS.
- Vashishth, V., Karak, B.B., Kitchatinov, L.: 2021, Subcritical dynamo and hysteresis in a Babcock-Leighton type kinematic dynamo model. *Research in Astronomy and Astrophysics* **21**, 266. DOI. ADS.
- Vashishth, V., Karak, B.B., Kitchatinov, L.: 2023, Dynamo modelling for cycle variability and occurrence of grand minima in Sun-like stars: rotation rate dependence. *Mon. Not. R. Astron. Soc.* **522**, 2601. DOI. ADS.
- Vidotto, A.A., Gregory, S.G., Jardine, M., Donati, J.F., Petit, P., Morin, J., Folsom, C.P., Bouvier, J., Cameron, A.C., Hussain, G., Marsden, S., Waite, I.A., Fares, R., Jeffers, S., do Nascimento, J.D.: 2014, Stellar magnetism: empirical trends with age and rotation. *Mon. Not. R. Astron. Soc.* **441**, 2361. DOI. ADS.
- Wilmot-Smith, A.L., Nandy, D., Hornig, G., Martens, P.C.H.: 2006, A Time Delay Model for Solar and Stellar Dynamos. *Astrophys. J.* **652**, 696. DOI. ADS.
- Wright, J.T.: 2016, Stellar Magnetic Activity Cycles, and Hunting for Maunder Minimum-like Events among Sun-like Stars. *AGU Fall Meeting Abstracts*, SH43D. ADS.